Direction of Oceanographic Vessel and Submarine Intervention
Underwater Systems Department

A.G. Allais

20/01/05 – DOP/CM/SM/PRAO/05.015

Project Exocet/D

Deliverable N° 2D1
Report on automatic lighting condition methods

Diffusion:
P.M. Sarradin DOP/CB/EEP/LEP
M. Perrier DOP/CM/SM/PRAO

☐ Confidential

☐ Restricted

☒ Public

Date	: 20/01/05	Number of pages	: 22
Reference	: DOP/CM/SM/PRAO/05.015	Number of figures	:
Analytic N°	: 850501	Number of annex	:
Contract N°	:	File name	: 2D1_05-015.doc
		Writer	: AGA

Subject/Title:

Project Exocet/D

Deliverable N° 2D1

Report on automatic lighting condition methods

Abstract:

Key-words:

Revisions

Grade	*Object*	*Date*	*Written by*	*Checked by*	*Approved by*
A	Creation	20/01/05	A.G. Allais		

TABLE OF CONTENTS

1. INTRODUCTION

Any image taken by an optical system presents some artefacts more or less important, such as geometric aberration (distortion), chromatic aberration or halo. The latter can be due to the optical system itself but also to the lighting. This phenomenon can be found on underwater images since photos or videos are acquired using artificial lighting.

This results in a non-uniform lighting within the images, which can have negative effects. For example, some algorithms can be applied to the image to detect some objects. If there is a halo within the image, the chance to detect the same object in different parts of the image is not equal. In some extreme cases, one object can be detected in one part of the image whereas it can go completely unnoticed in another part of the image. The non-uniformity of lighting has an obvious impact on the mosaic creation process as well. In the simplest case of matching two images together, the first image is considered as the reference image, the second one is the image to match. The method consists of detecting point features in the first image and matching them with the same features in the second image. As we said before, if there is a lighting halo within the images, some points can be detected only in one image or can be mismatched. But, this can be overcome by selecting only well matched points. However, the result is not good because the two images are juxtaposed and one region of the first image can be close to one region darker in the second image. This results in a discontinuity in the final image, which is not satisfactory.

In this report, we have only taken an interest in the correction of lighting within images. The study we have led presents the causes of the non-uniform lighting and then aims at reducing the negative effect of the non-uniform lighting. Two methods have been investigated. The first one is based upon the reflectance-illumination modelling of the image and the second consists of a radiometric correction.

2. CAUSES OF NON-UNIFORM LIGHTING

The non-uniform lighting is due to several factors. Some of them are presented hereafter. But, firstly, several notions of optics have to be explained.

2.1. *Definition*

The «luminance» is the luminous flux (quantity of luminous energy) that is emitted by an area.

The «illuminance» is the luminous flux that is received by an area.

2.2. *Non-uniformity due to the optical system*

According to photometry, it is well-known that the «illuminance» of a physical imaging system consisting of a surface area of constant «luminance» varies with the angle between the optical axis and the principal ray passing through the observation point. This is given by the following relationship and illustrated by Figure 1:

$$E(x,y) = E_0 \cos^4 \Phi \qquad (2.1)$$

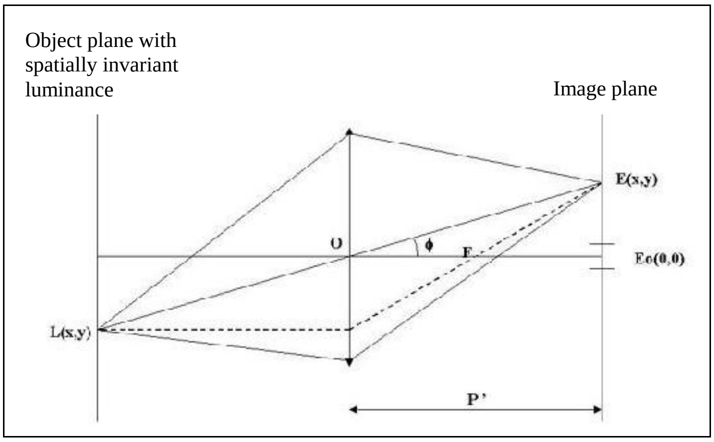

Figure 1: Image «illuminance» as a function of object «luminance»

This result indicates that the «illuminance» decreases when the angle Φ increases. Thus, the image corners are always darker than the centre of the image. This first phenomenon can imply a non-uniform lighting in the images, and it is visible when the optical system is wide-angle.

In case of video mosaicing, the camera is roughly perpendicular to the object surface so this phenomenon is not very important.

2.3. Non-uniformity due to the lights

In addition to the optical system itself, the light sources that are used to get good images in an underwater environment contribute also to the non-uniformity. Indeed, in order to simplify, in case of a single source, the «illuminance» of a surface varies with the angle between the normal axis and the light ray.

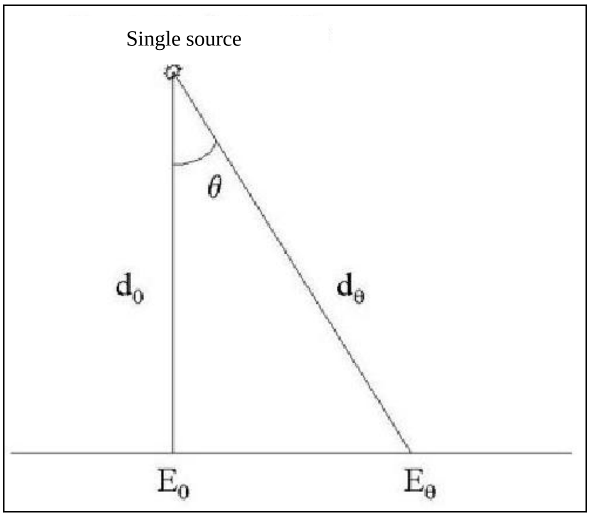

Figure 2: Surface «illuminance» by a single source

The mathematical relationship is given by:

$$E_\theta = E_0 \cos^3 \Theta \qquad (2.2)$$

This implies that, even if an object has a uniform «luminance», if this object is not in the centre of the light field, it will be seen by the camera as an object with a non-uniform «luminance».

In most cases in an underwater environment, the lights are fixed next to the camera so the angle Θ is not equal to zero. As a result, this phenomenon is significant and must be taken into account.

2.4. Light absorption as a function of the depth

Light intensity decreases in relationship to distance. This phenomenon is directly linked to the water absorption. Let's consider the sunlight on the sea surface, the light intensity I_λ for a given wavelength λ decreases as a function of depth z:

$$I_\lambda(z) = I_{0,\lambda} e^{-k_\lambda z} \quad (2.3)$$

In this formula, vertical attenuation coefficient of water k_λ is a function of wavelength λ. Thus attenuation is different according to wavelength. In Figure 3, it can be seen that attenuation depends on the wavelength and of the water quality (clear in full line or turbid in dashed line). In case of clear water, red is more attenuated than blue, that's why in water, the scenes tend to be blue.

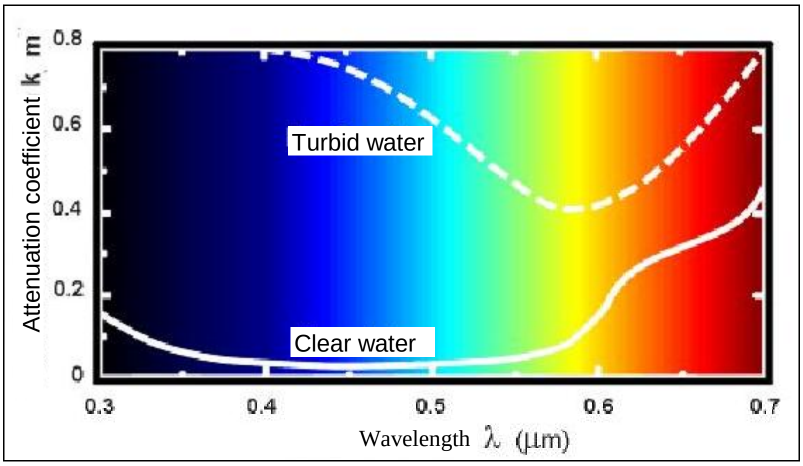

Figure 3: Water vertical attenuation coefficient relative to wavelength

This leads to the next figure on which the light energy is represented for different depths relative to wavelength. It is of course dependent on the water quality. Given the fact that video and photo applications are carried out when water is clear, these curves show that the light energy at a given depth is not equal for all wavelengths. So, this fact should be taken into account for lighting correction of colour images.

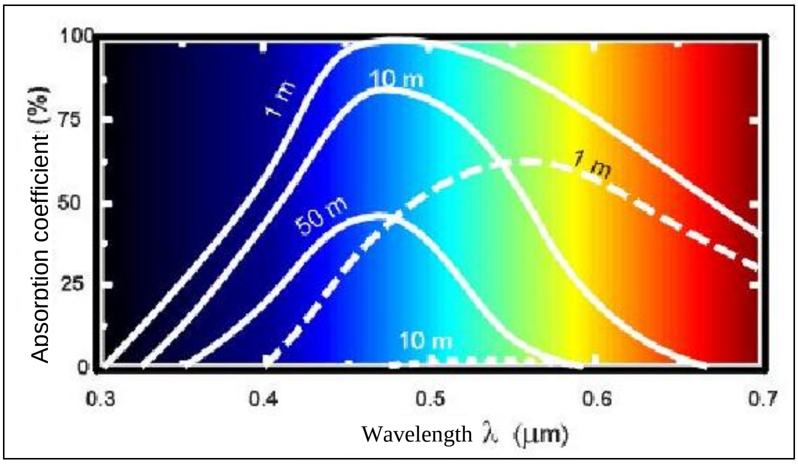

Figure 4: Absorption coefficient relative to wavelength

3. METHODS

The different causes for non-uniform lighting in images, led us to correct the images considering physical phenomena and not only by using simple image processing methods, such as local contrast enhancement. So, the algorithms we present hereafter rely on the previous physical notions we have presented.

3.1. Radiometric correction

3.1.1. Theoretical modelling

First of all, besides the radiometric causes («luminance», …), some artefacts in the image originate in the sensor itself. The cameras we use in an underwater environment often have a CCD sensor and we assume that CCD cells have the same sensitivity and the same radiometric response. In fact, that is not so and the system has to be corrected regardless of the scene and the lighting. It is generally quite difficult to model the pixel faults and we are led to use reference images to calibrate each pixel separately.

To begin with, we must understand how images are recorded by a CCD camera. CCD's consist of area arrays of small spots of silicon. When light strikes the array, electrons are released from each silicon spot in proportion to the quantity of light falling on the spot. The charge released by each spot (the intensity current) is measured and makes it possible to build the image. When receiving light, the CCD cell response is proportional to the silicon thickness. But there will always be slight inaccuracy causing variation in cell response and, as a result, in image quality. This variation may be modelled by variable g^i_{sens} distinctive for each pixel *i*.

Moreover, the current emitted by the CCD array when no light is received may vary up to 10 % across the pixels. This phenomenon is modelled by variable I^i_{dark} .

In addition, the transmission between the camera and the acquisition card is noisy. This noise can be modelled as a centred and independent noise I^i_{transm} .

And finally, as we explained before, there is a variation due to the optical system itself (light intensity varies as a function of $\cos^4 \Phi$). When the optical system is a real one, the effect is much more important. The light intensity can vary by 10% between the image centre and the borders. This effect is modelled by variable g^i_{opt}.

The global mathematical modelling for such radiometric variations in images is given by:

$$I^i_{real} = g^i_{sens} g^i_{opt} I^i_{ideal} + I^i_{dark} + I^i_{transm} \tag{3.1}$$

With:

- I^i_{real} : pixel value read in the image,
- I^i_{ideal} : pixel value if the image had been ideal, without any perturbation,
- I^i_{dark} : pixel value when no light is received,
- I^i_{transm} : pixel value when there is only noise due to transmission,
- g^i_{sens} : factor modelling the variation of sensitivity between pixels,
- g^i_{opt} : factor modelling the variation of light due to the optical system.

So, $g^i_{sens} g^i_{opt}$ is the image pixel value, to a scale factor, when the CCD cell is uniformly lit up.

As a result, we obtain the corrected, ideal image:

$$I^i_{ideal} = \frac{I^i_{real} - I^i_{dark} - I^i_{transm}}{g^i_{sens} g^i_{opt}} \tag{3.2}$$

3.1.2. Experimental modelling

For radiometric correction, the goal is to find the good images which are used in Eq. (3.2). in order to simplify the model, we can assume that the transmission noise is equal to zero. We can also make the hypothesis that the image when no light is received is equal to zero. We then only keep the term of variations due to the optical system and to the sensor.

The simplified equation becomes:

$$I^i_{ideal} = \frac{I^i_{real}}{g^i_{sens} g^i_{opt}} \tag{3.3}$$

3.2. Homomorphic filtering

The second method we investigated is homomorphic filtering. This method is a generalized technique for image enhancement and/or correction. It simultaneously normalizes the brightness across an image and increases contrast.

The theory behind homomorphic filtering relies on the fact that an image $f(x,y)$ can be expressed as the product of illumination $i(x,y)$ and reflectance $r(x,y)$:

$$f(x,y) = i(x,y)r(x,y) \qquad (3.1)$$

Homomorphic filtering consists of separating illumination and reflectance. Indeed, illumination tends to vary slowly and steadily across an image whereas reflectance tends to vary sharply, especially at object borders. The aim of homomorphic filtering is then to process separately low frequencies, which stand for illumination and high frequencies, which represent the reflectance. The steps are presented hereafter.

First, take the Naperian logarithm of $f(x,y)$:

$$\ln f(x,y) = \ln i(x,y) + \ln r(x,y) \qquad (3.2)$$

Let's now apply the Fourier transform:

$$F(u,v) = I(u,v) + R(u,v) \qquad (3.3)$$

where $F(u,v)$ is the Fourier transform of $f(x,y)$, $I(u,v)$ is the Fourier transform of $i(x,y)$ and $R(u,v)$ is the Fourier transform of $r(x,y)$.

Now, we can apply filter $H(u,v)$ to $F(u,v)$:

$$F(u,v)H(u,v) = I(u,v)H(u,v) + R(u,v)H(u,v) \qquad (3.4)$$

In this relation, we can see that, if the filter is well chosen, it can process high and low frequencies independently. Low frequencies lie in the centre of the Fourier spectrum whereas high frequencies are located at the borders. For the lighting correction application, the filter aims, on one hand, at attenuating low frequencies to remove the halo in the image due to non-uniform lighting, and on the other hand, increasing high frequencies in order to enhance the contrast. Therefore, by applying a frequency domain filter, we can reduce intensity variation across the image while highlighting detail.

So, only high pass filters are adapted to our application. Some of them are represented in the following figures.

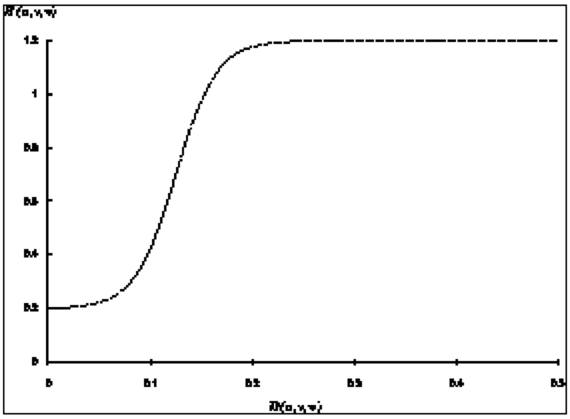

Figure 5: Cross section of a spherically symmetric homomorphic filter as a function of the distance from the origin

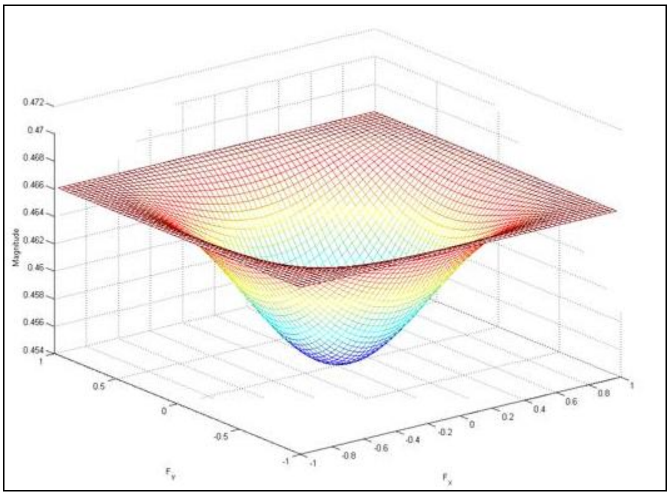

Figure 6: Example of a homomorphic filter in 2D

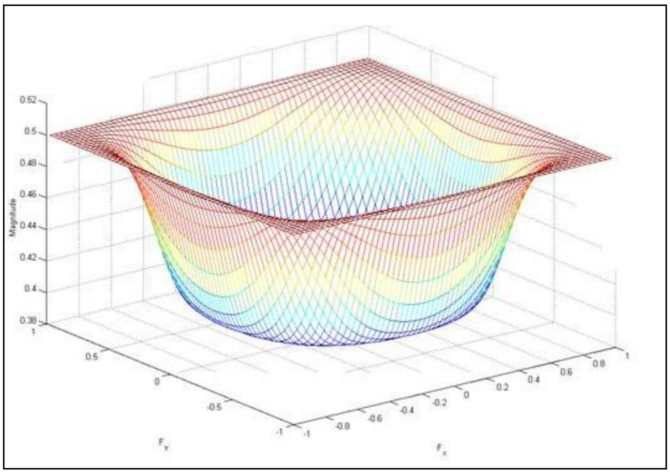

Figure 7: Example of an homomorphic filter in 2D

Once the filter has been applied in the Fourier domain, the inverse Fourier transform and the exponent operator are processed to get the final corrected image $f'(x,y)$:

$$f'(x,y) = i'(x,y)r'(x,y) \tag{3.5}$$

Now, $i'(x,y)$ and $r'(x,y)$ are the illumination and reflectance of the enhanced image.

This global approach may be summarized in Figure 8 (DFT is the Discrete Fourier Transform and IDFT is the Inverse DFT).

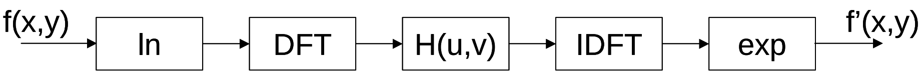

Figure 8: Homomorphic block diagram

4. RESULTS

4.1. Homomorphic filtering

The first part of our study aims at selecting a good filter for the images. As we said before, the filter must be a high pass filter since it must attenuate low frequencies while enhance high frequencies.

Two shapes of filter available in Matlab™ have been tested. The first one is function fir2, and the second is function remez. They can be designed by adjusting some parameters, which are the cut-off frequency (Fc), the amplitude (A) and the order (O). The cut-off frequency correspond to the frequency at which the filter starts to have an effect, i.e. for a high pass filter, the filter will attenuate frequencies which are under the cut-off frequency. The order is used to design the slope of the filter around the cut-off frequency and the amplitudes are defined for each frequency.

In the following sections, we briefly survey the results of parameter optimisation for the filters. This optimisation is based on visual effect although we could use criteria such as the average and the standard deviation. Several results are also presented on underwater images.

4.1.1. Matlab™ Fir2 function

Function fir2 is a frequency sampling-based finite impulse response filter.

The parameters we have chosen to begin with are the following: O = 2, Fc = 0.2, A = [0.3 0.3 0.5 0.5].

The order has been modified to see the effect on the images. The results are presented in the following table. We can see that this parameter is not very critical since the orders from 2 to 6 are suitable.

Order	Visual effect
2, 4, 6	Good
8, 10, 12	Dark images with little contrast

Table 1: Filter order study for fir2

Next, the order has been set up to 2 and the frequency has been modified. In fact, the frequency is a normalized frequency varying from 0 to 1. The results are shown in Table 2. Even if several frequencies give quite good results, a cut-off frequency of 0.2 is better. So, we have chosen this value for the next study.

Cut-off frequency	Visual effect
0.1	Slightly dark
0.2	Good, with good contrast
0.3, 0.4, 0.5, 0.6	Acceptable
0.7	Slightly too much luminous
0.8	Very luminous

Table 2: Cut-off frequency study for fir2

So, now, the frequency characteristic is [0 0.2 0.2 1] (frequencies range from 0 to 1 with a cut-off frequency of 0.2) and the amplitudes must be designed for these frequencies. The amplitude characteristics are defined by one value for frequencies from 0 to 0.2 and one value for frequencies from 0.2 to 1. Several results are presented in Table 3. The best result is obtained with values of 0.3 and 0.5.

Amplitude characteristics	Visual effect
0.1 – 0.3 to 0.5	Very luminous with little contrast
0.3 – 0.5	Good
0.5 - 0.7	Dark
0.5 - 0.7 to 0.9	Dark

Table 3: Amplitude study for fir2

Finally, the global shape of the optimised filter is represented in Figure 9.

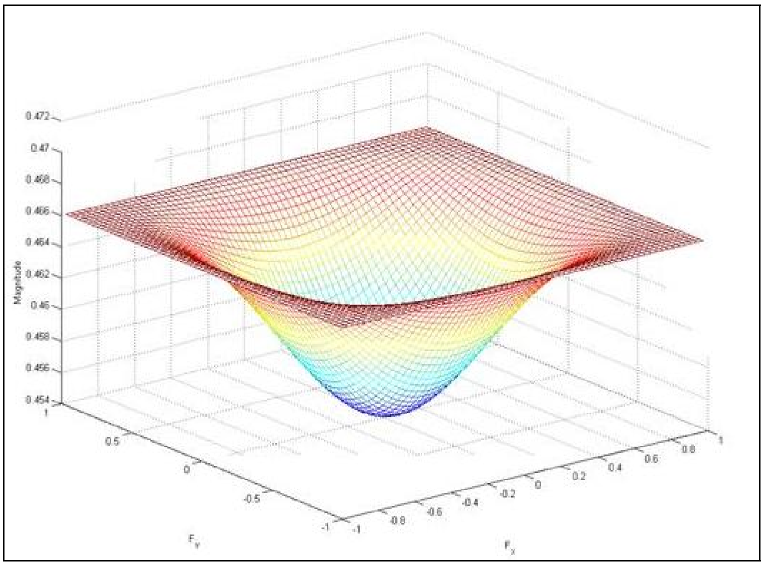

Figure 9: Filter generated by Matlab function fir2 – O = 2, Fc = 0.2, A = [0.3 0.3 0.5 0.5]

The results obtained on three underwater images of amphorae are shown in Figure 10. On the left part, we can see the original images and on the right, the filter has been applied to original images. On the filtered images, the halo of light intensity has been attenuated while the details are still visible.

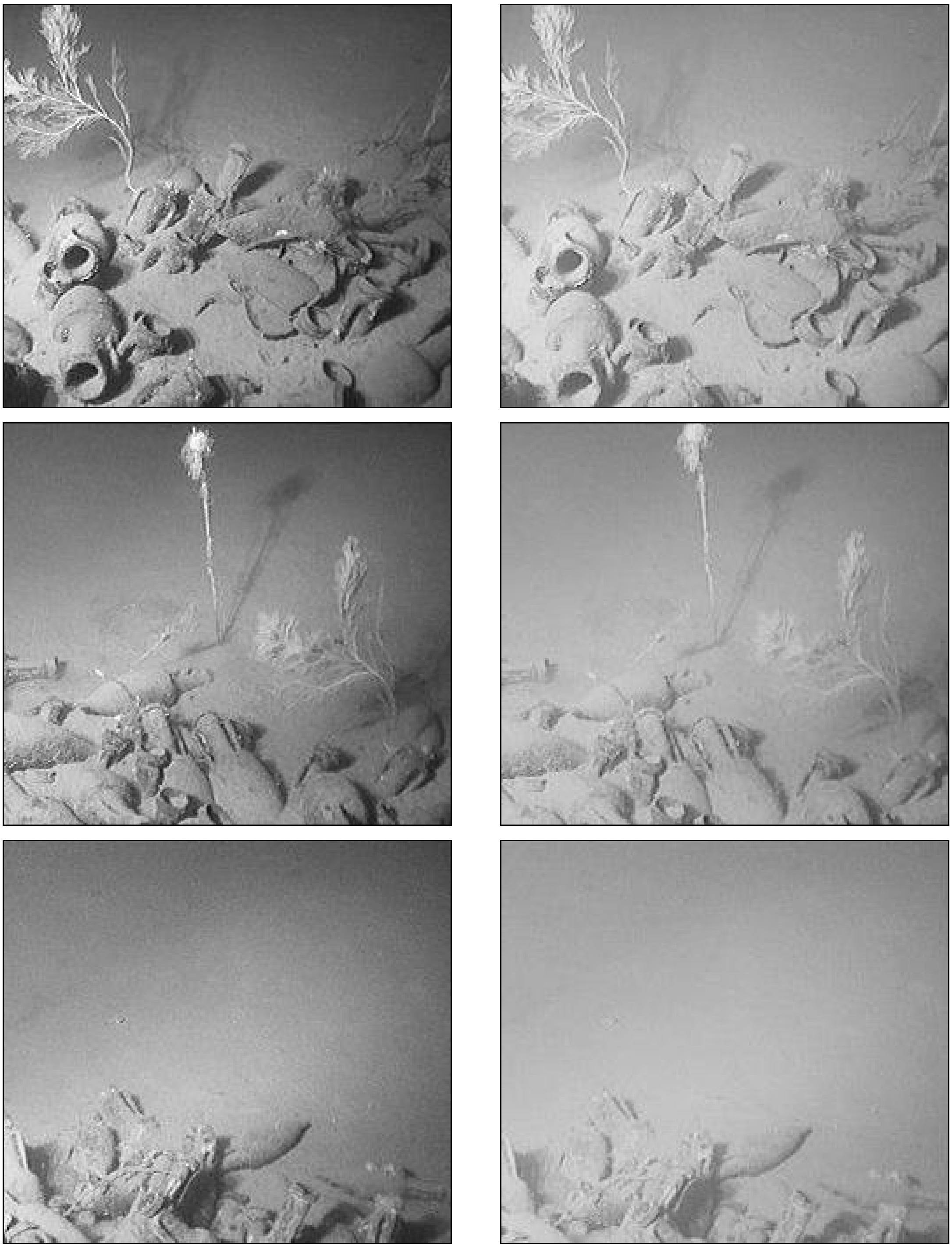

Figure 10: Result of fir2 filter on three images.
The original images are on the left. The filtered images are on the right.

4.1.2. Matlab™ Firpm function

We have proceeded the same way for the other filter. Function firpm is a linear-phase finite impulse response filter using the Parks-McClellan algorithm. The Parks-McClellan algorithm designs filters with an optimal fit between the desired and actual frequency responses. The filters are optimal in the sense that the maximum error between the desired frequency response and the actual frequency response is minimized.

Firpm exhibits discontinuities at the head and tail of its impulse response so the desired amplitude at the cut-off frequency is unspecified. The area around this point is a transition region.

O is the order of the filter and vectors F and A specify the frequency-magnitude characteristics of the filter.

The optimised filter for our application has the following characteristics:

- O = 20
- F = [0 0.75 0.8 1]
- A = [0.4 0.4 0.5 0.5]

The desired amplitude at frequencies between 0 and 0.75 is 0.4 and the desired amplitude at frequencies between 0.8 and 1 is 0.4. The desired amplitude at frequencies between 0.75 and 0.8 is unspecified.

The filter is shown on Figure 11.

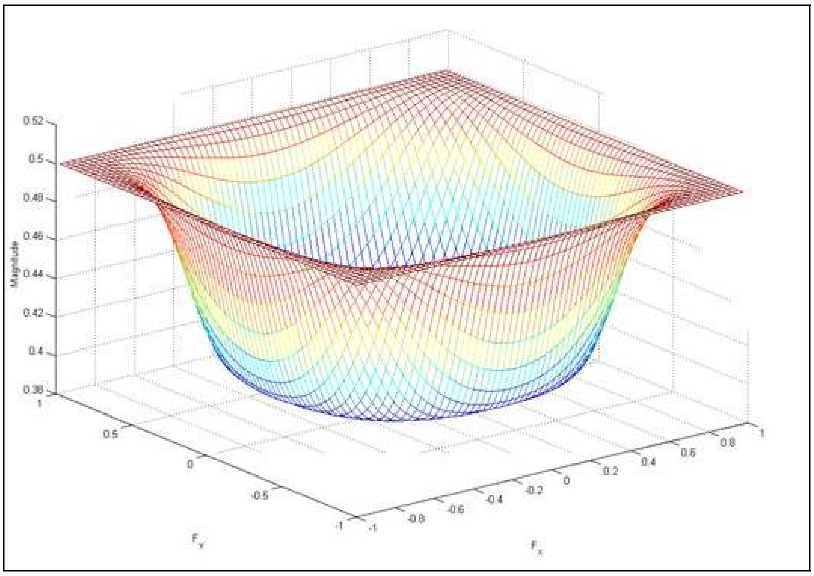

Figure 11: Optimised firpm filter – O = 2, F = [0 0.75 0.8 1], A = [0.4 0.4 0.5 0.5]

The results obtained on amphorae images are shown on Figure 12. It can be seen that the halo due to the lighting is reduced and the details are still found.

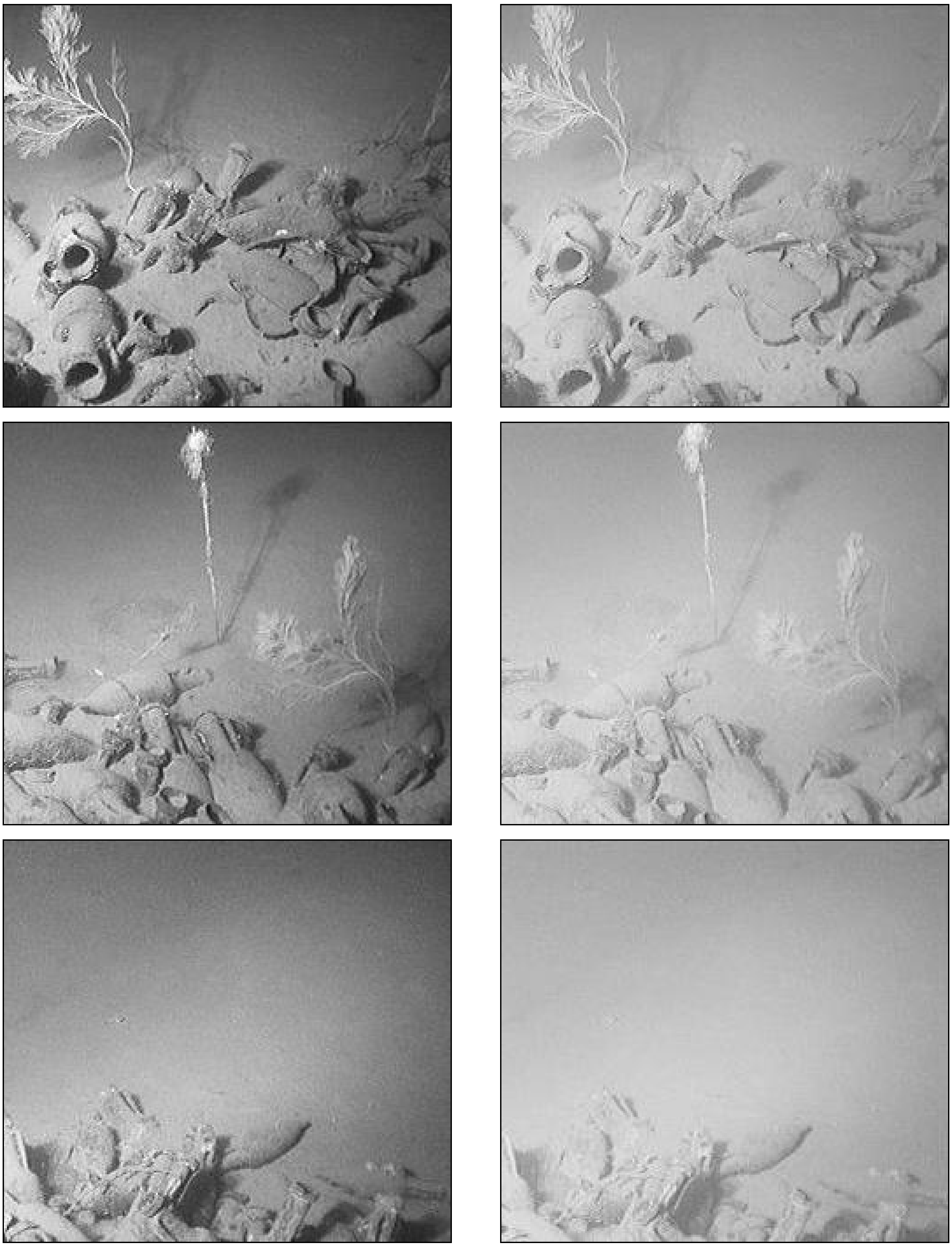

Figure 12: Result of firpm filter on three images.
The original images are on the left. The filtered images are on the right.

4.2. Radiometric correction

This method requires a reference image that is taken with lights and no object. We don't have this kind of image for the images we can use. So, first of all, we have applied this method to images taken with a webcam in the air. Two images are acquired with no object but only lights to obtain the image of «luminance» variation (Figure 13). Afterwards, one object is put in the webcam field in different places (Figure 14). The images with objects are then corrected using the images of «luminance» variation (Figure 15 and Figure 16). In these images, it can be seen that the «luminance» is corrected well. But, before going further, both methods have to be compared with the same images.

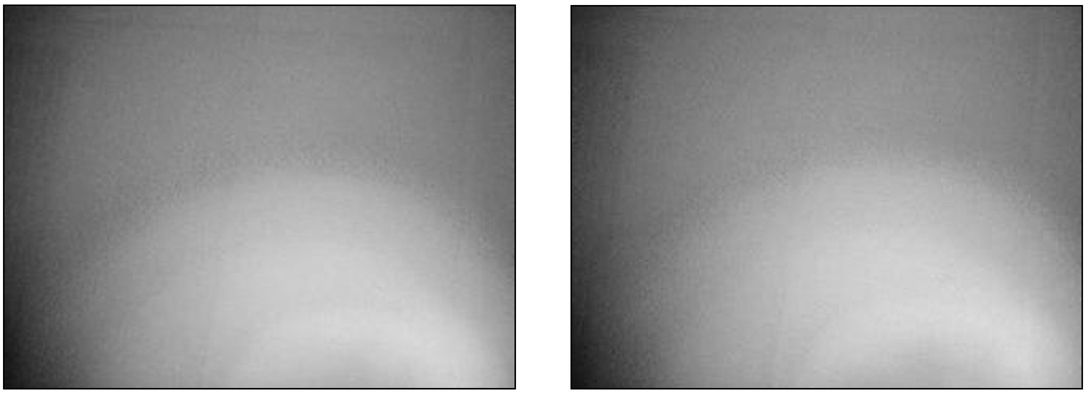

Figure 13: Two reference images (Ir1 and Ir2)

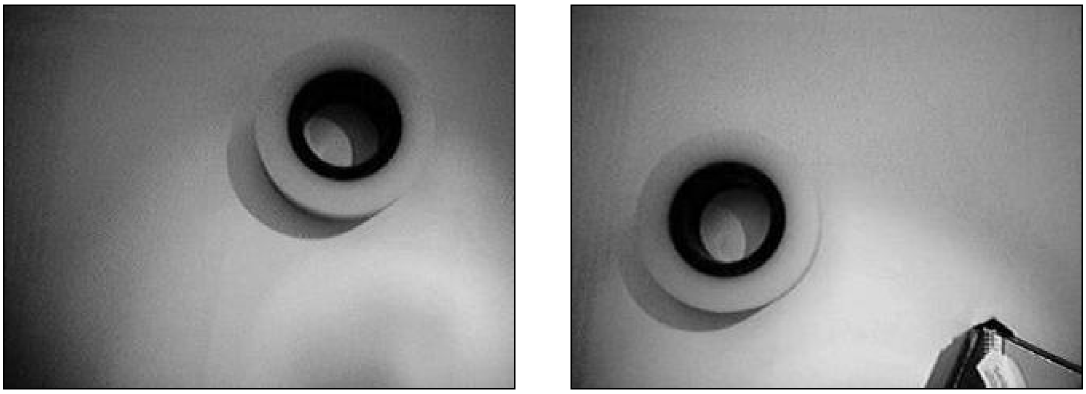

Figure 14: Original images I1 and I2

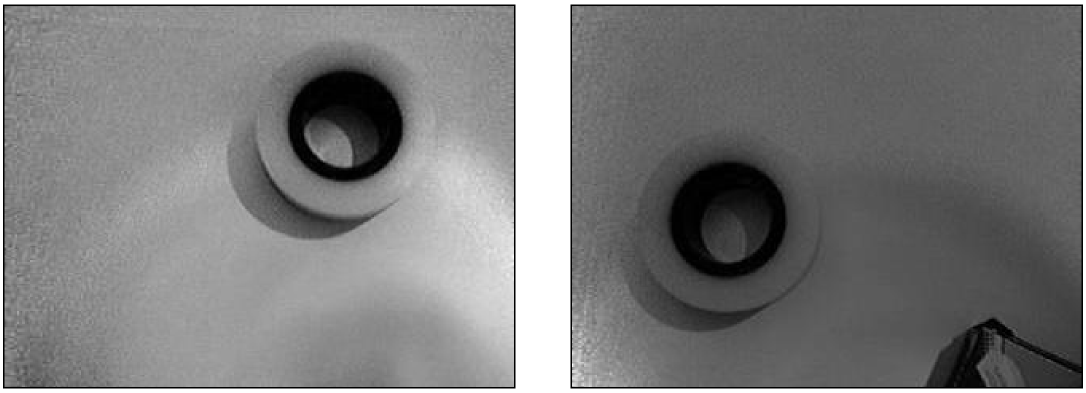

Figure 15: Images I1 (left) and I2 (right) corrected with Ir1

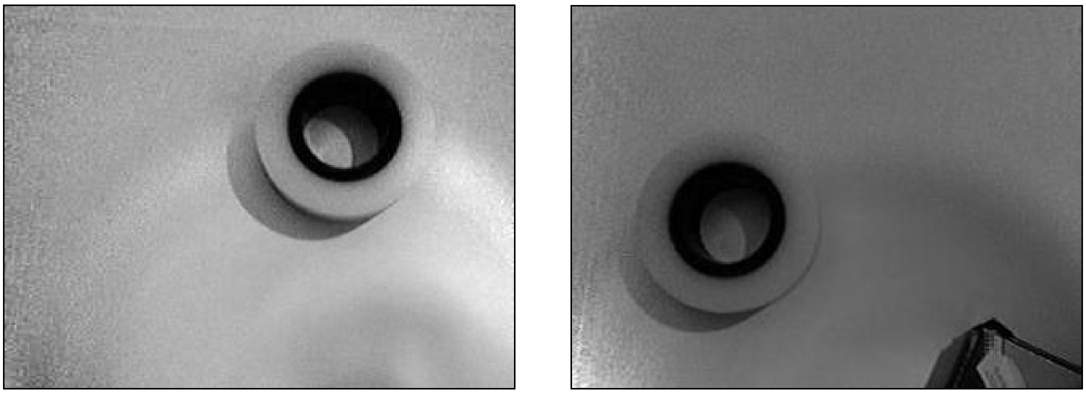

Figure 16: Images I1 (left) and I2 (right) corrected with Ir2

4.3. Comparison

In this section, homomorphic filtering and radiometric correction are compared using the same images. The results are presented in Figure 17, Figure 18 and Figure 19.

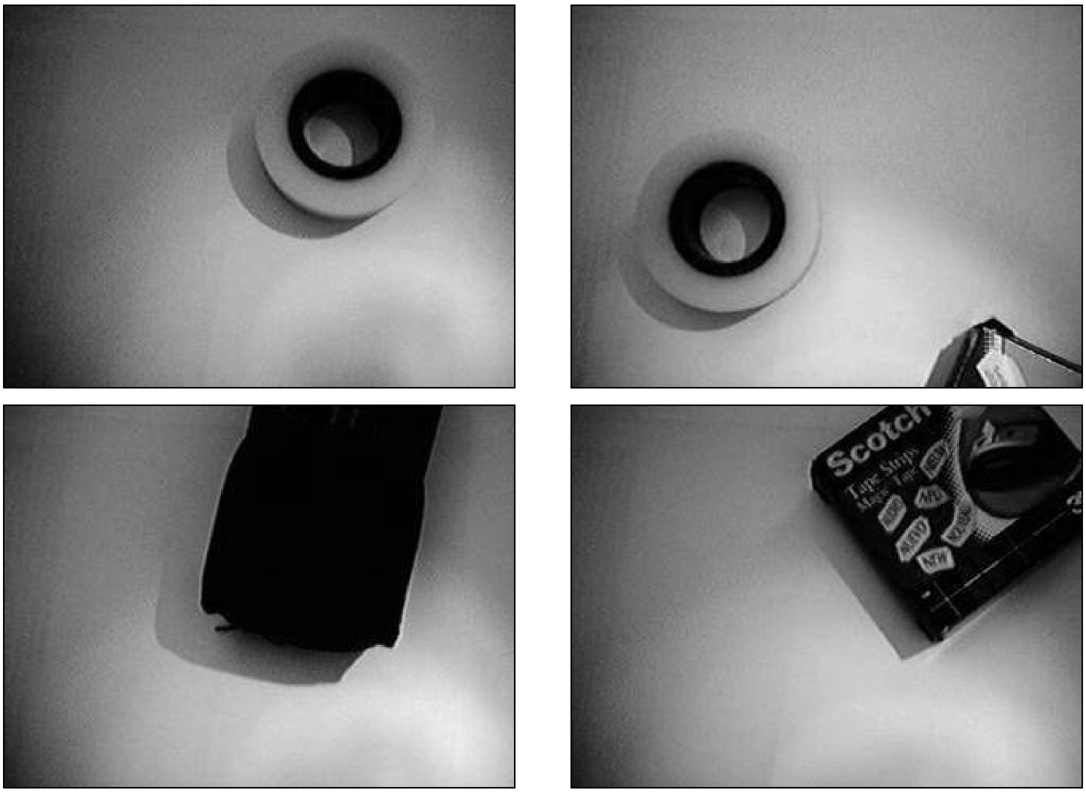

Figure 17: Original images I1, I2, I3 and I4

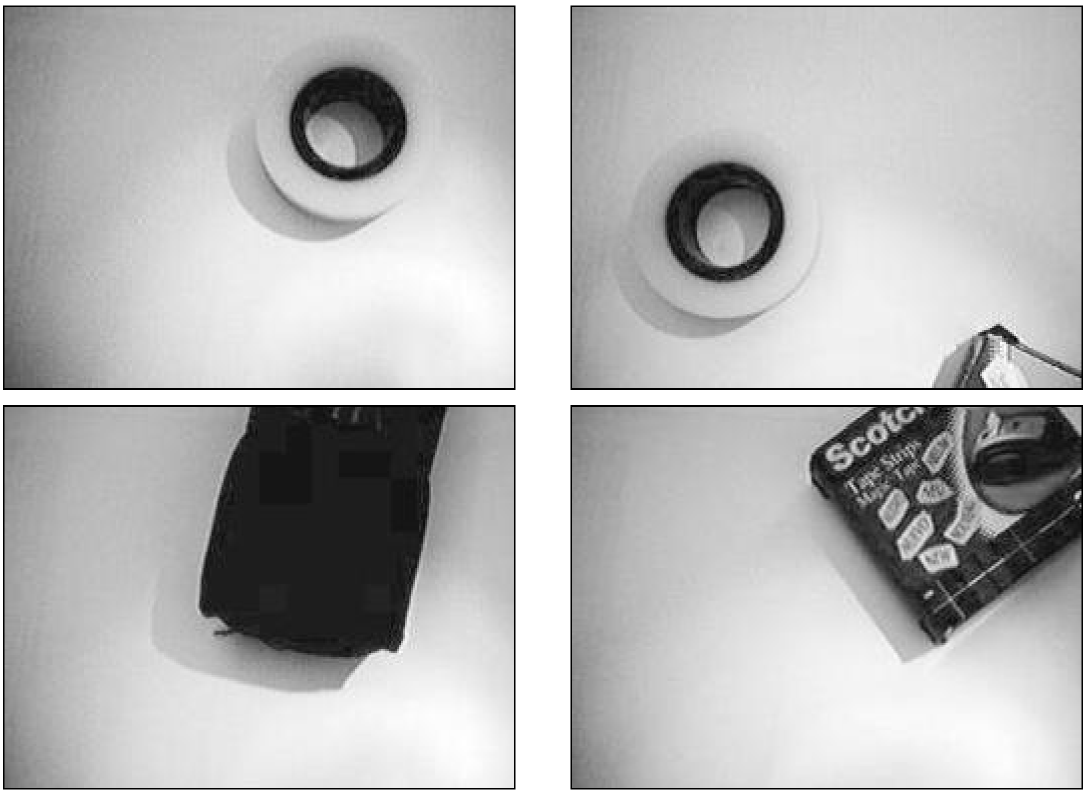

Figure 18: Images I1, I2, I3 and I4 corrected by homomorphic filtering (function fir2)

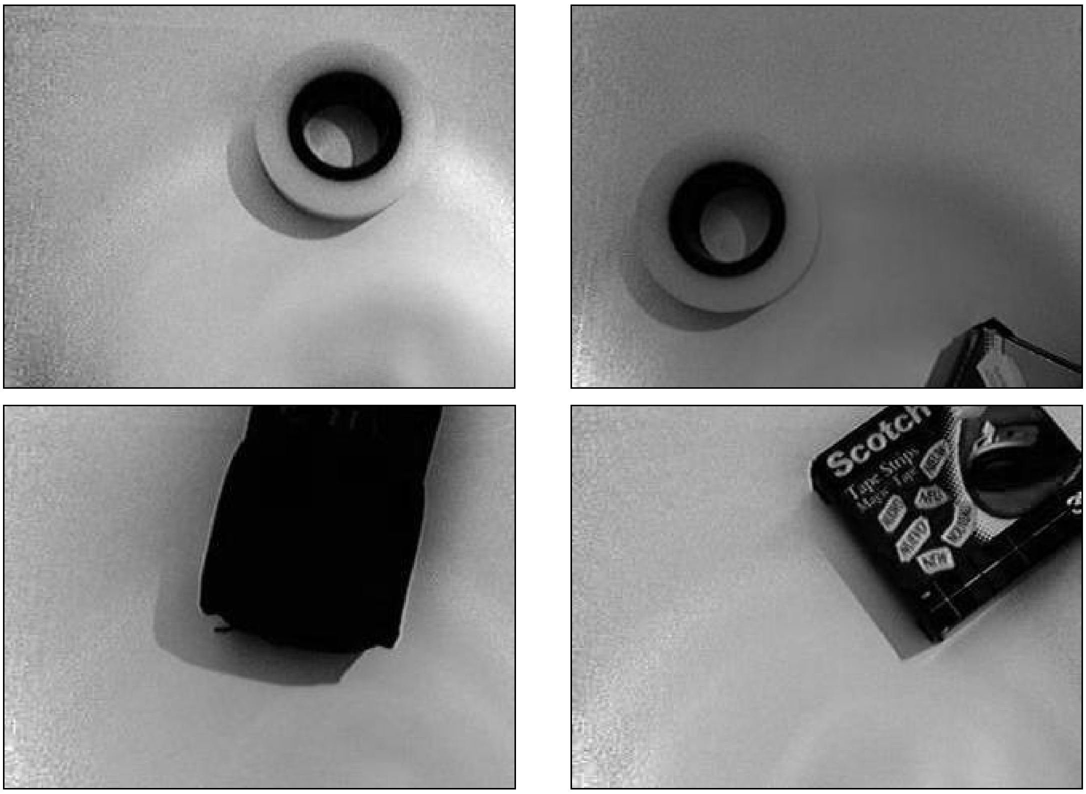

Figure 19: Images I1, I2, I3 and I4 corrected by radiometric method

In these images, it can be clearly seen that the non-uniform lighting is far less important in the images corrected by the radiometric method. Although the images seem to be noisier than images corrected by homomorphic filtering, they are sharper and less blurred.

Moreover, the method of radiometric correction can be carried out more easily. It consists only of a division whereas the homomorphic filtering requires to work in the Fourier domain. Besides, the optimal filter is determined only experimentally. The radiometric correction uses a physical image which represents the non-uniform lighting.

As a conclusion, the radiometric correction is the most promising method provided that the reference image is given. Only one image has to be acquired before the image sequence acquisition. No further processing is needed to use this reference image, resulting in a simple operational procedure on the ROV. In the following section, we survey several methods to acquire the reference image.

4.4. Application of radiometric correction to underwater images

For the examples, the underwater images have been acquired with no reference image so it is rather difficult to apply the radiometric correction. However, we have made some tests with a reference image acquired on the open sea while diving. The lighting is not the same as the one used on the images of the seabed but it can even be interesting to analyse the results.

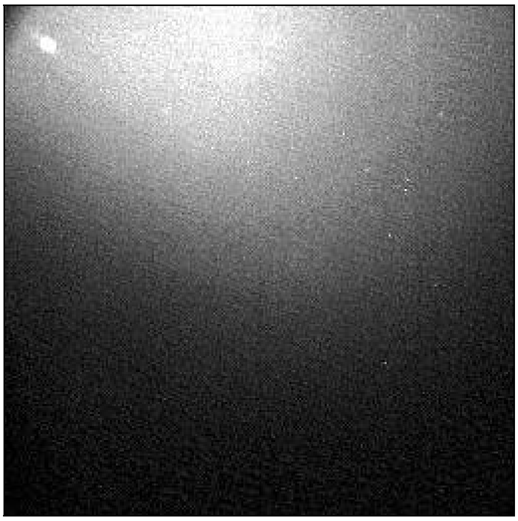

Figure 20: Reference image

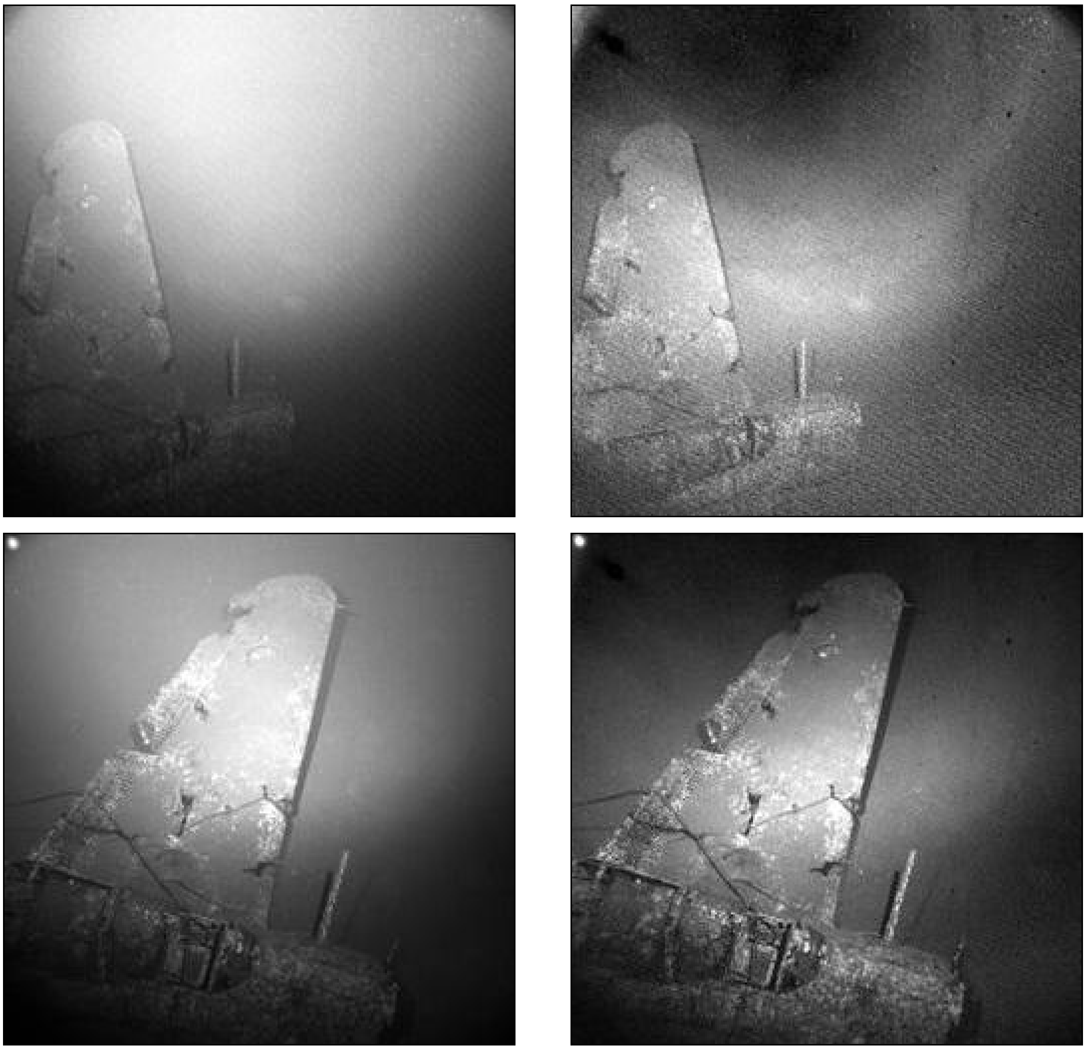

Figure 21: Original images (left) and corrected images (right)

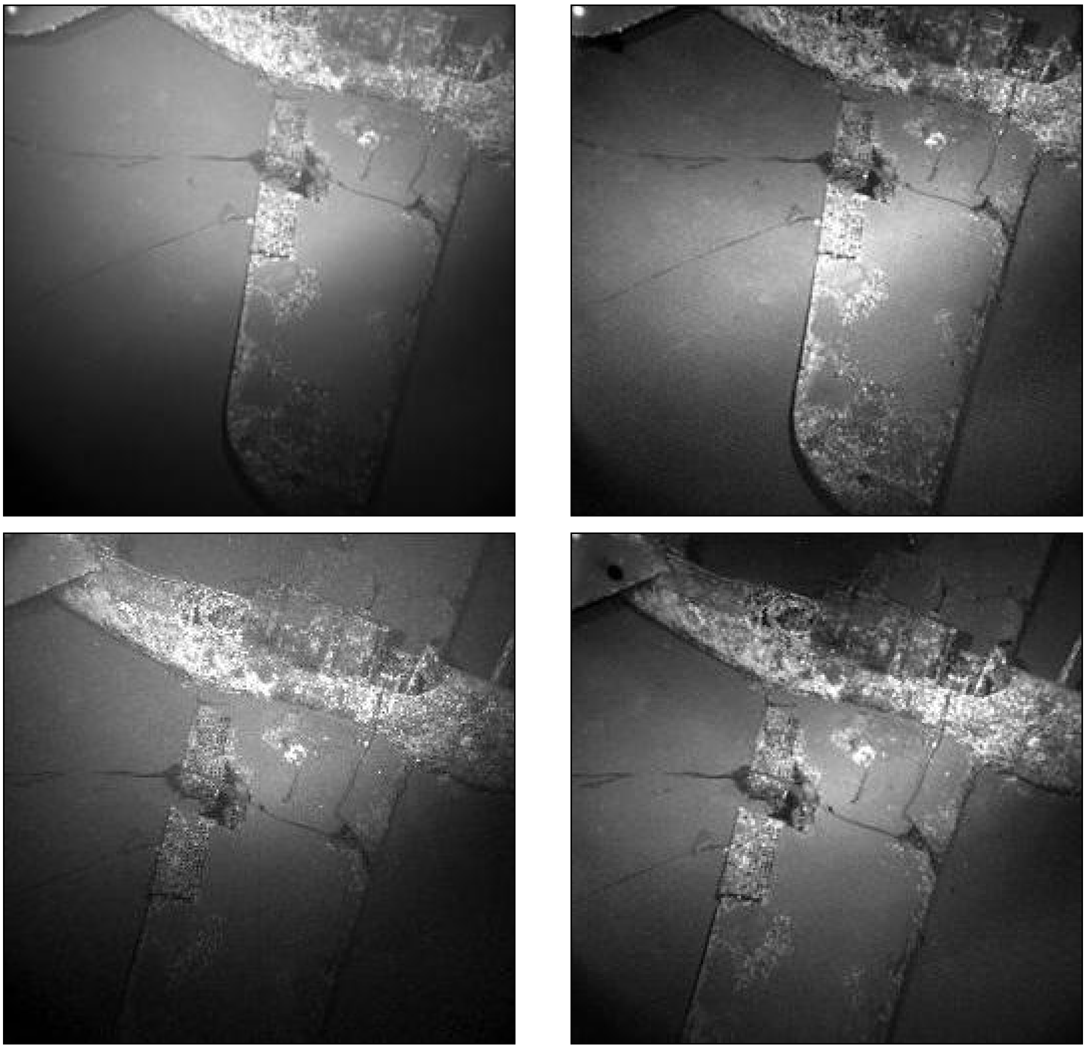

Figure 22: Original images (left) and corrected images (right)

First of all, it can be seen that the halo in the reference image is less large than in the images with the airplane. It is normal because the conditions were not the same. So, except in the centre where a slight halo is still visible, the images are corrected very well. In the lower left hand corner and in the upper half of the images, the details of the airplane and of the wing are enhanced. We can imagine that if the reference image had been taken in the same conditions (at least, same position of lights and camera), the results would have been even better.

Another means to obtain the reference image could be to tune up the focal to infinity and to take an image of the seabed. But, by this way, the seabed needs to be flat, homogeneous with no object. So the way consisting of acquiring one image while diving seems to be the simplest way to proceed.

4.5. *Extension of the radiometric correction to colour images*

To apply the radiometric correction to colour images, the RGB (Red-Green-Blue) images can be converted into YUV images. In this format, the «luminance» and the chrominance are encoded in different components. Y is the «luminance», U and V are the chrominance components. The interest to separate these two components is to apply the correction only to the «luminance» component of the colour image.

Several transformation matrices can be found to operate the RGB-YUV conversion. The matrix represents the relationship between the «luminance», the chrominance and the colour components. The «luminance» is the weighted sum of the different colour components and the different weights reflect the differences in the human eye's response to different wavelength of light. U and V components are known as Colour Difference values and represent a relative distance from a zero saturation point in a colour coordinate space along two perpendicular axes. The different coefficients are deduced from experiments that's why they can vary according to the experiment protocols and the norms.

The most commonly used relationship is the relationship defined by the CCIR-601 norm. This relationship is also used in the JPEG norm.

The relationship is:

$$\begin{cases} Y = 0.299R + 0.587G + 0.114B \\ U = 0.564\,(B - Y) \\ V = 0.713\,(R - Y) \end{cases}$$

With the matrix notation, it gives:

$$\begin{bmatrix} Y \\ U \\ V \end{bmatrix} = \begin{bmatrix} 0.299 & 0.587 & 0.114 \\ -0.1687 & -0.3313 & 0.5 \\ 0.5 & -0.4187 & -0.0813 \end{bmatrix} \begin{bmatrix} R \\ G \\ B \end{bmatrix} + \begin{bmatrix} 0 \\ 128 \\ 128 \end{bmatrix}$$

And the inverse matrix is:

$$\begin{bmatrix} R \\ G \\ B \end{bmatrix} = \begin{bmatrix} 1 & -0.0003682 & 1.4019876 \\ 1 & -0.3441133 & -0.7141038 \\ 1 & 1.7719781 & -0.0001346 \end{bmatrix} \begin{bmatrix} Y \\ U - 128 \\ V - 128 \end{bmatrix}$$

5. CONCLUSION

As a conclusion, we can say that the lighting conditions in an underwater environment depend on several parameters which cannot be necessarily overcome, such as the quality of water. As a result, several methods have been investigated to correct the images and have been tested on black and white images. The radiometric correction seems to be the most promising. It can easily be applied since it consists only of a division of the image by a reference image and the results are very good. Moreover, it can be easily transposed to colour images as soon as the RGB image is converted into a format where the «luminance» component is separated from the other components, such as the YUV format.